

## SCIENTIFIC REPORT 2015

### Microfluidic multiple cell chip platform for biotransformations of phenylalanine analogs with covalent immobilized PAL on magnetic nanoparticles

Microfluidic application of immobilized enzymes offers novel possibilities in diagnostics, synthetic or analytical applications. When PAL is immobilized in magnetic nanoparticles (MNPs), the MNPs are applicable to flow in microfluidic systems together with the liquid, or can be anchored at pre-designed positions so that the flow of the fluid in the system can be chosen freely compared to them. This creates a unique opportunity to develop modular micro-systems with the ability of flexible variation of biocatalysts Error! Bookmark not defined.

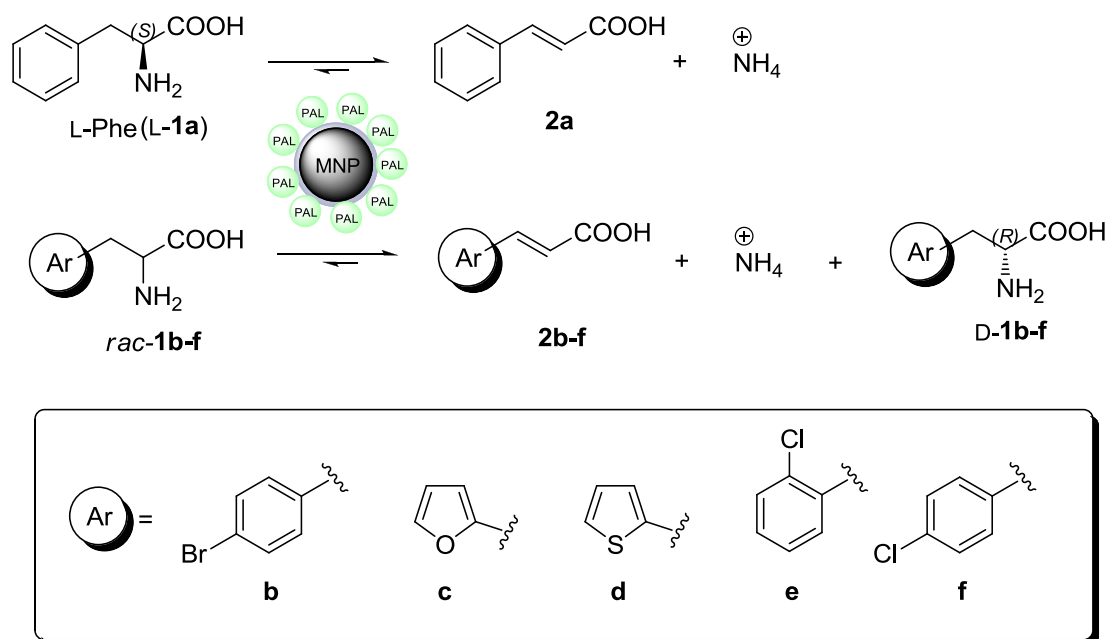
Magne-Chip is a microfluidic platform comprising the necessary fluid actuators (e.g. pumps, valves and thermostat) and sensors (e.g. pressure sensor), a flow controller and a microfluidic chip containing a number of microliter volume reaction chambers. The chambers are addressable selectively by a directed magnetic field, which makes possible the accumulation of MNPs from a previously selected MNP suspension in the selected chambers.

One of our objectives was to study the properties and parameter settings of the Magne-Chip system in biotransformations with PAL enzyme using the natural substrate L-phenylalanine (**L-1a**) and five unnatural amino acids (*rac-1b-f*) including DL-2-amino-3-(4-bromophenyl)propanoic acid (*rac-1b*) which has never been tested as substrate for PAL from *Petroselinum crispum* (PcPAL).

Reliability and reproducibility of the experiments performed with the Magne-Chip platform (Figure) on the natural substrate phenylalanine were analyzed experimentally, providing the basis of the in-chip biotransformation study with PAL-coated MNPs (referred as MNPs) acting on unnatural substrates (*rac-1b-f*, in Scheme 1). First, substrate flow rate and concentration were studied and optimized using L-phenylalanine **L-1a** as substrate. Then biocatalytic activity of the in-chip biotransformation with each unnatural amino acid (*rac-1b-f*) was determined and compared to the biocatalytic activity of L-phenylalanine **L-1a** which is the natural substrate of PAL enzyme as a reference.

When filling up the chip (see Section 4.2.4 in *Experimental*), the prepared MNP suspension was driven through the chip by applying a slight air pressure (0.2-0.3 bar) to the suspension vial connected to the inlet of Magne-Chip via a PTFE tube (Figure, *Chip filling*) while the temperature of the chip was kept on 25 °C. During the filling process, the MNPs

were accumulated in the reaction cells due to the permanent magnets placed in moveable drawers enabling “on/off” switching of the magnetic field. Once one cell was saturated (Figure 1), the magnet of the previous cell was turned on. The same procedure was repeated (Figure 1) until the required number of chambers was filled up. Each cell of the Magne-Chip device could capture ca. 250  $\mu\text{g}$  of MNPbiocatalys.



**Scheme 1**—Ammonia elimination from different amino acids (**1a-f**) catalyzed by PAL immobilized on MNPs

### Performing multi-parameter experiments in Magne-Chip

Once the Magne-Chip was filled with MNPs, the dosage of liquids flowing through the chip could be controlled in a programmed manner. As the MNP biocatalysts are reusable, the chip could be cyclically re-initialized by washing after each biotransformation experiment. This enabled the switching of the substrate or changing the working parameters cycle by cycle without changing the biocatalyst in the system i.e. screening conditions or various substrates following an automated sequence.

Magne-Chip experiments involved four steps: 1) filling up the chip with MNPs, 2) absorbance calibration 3) experiment cycles 4) chip cleaning.

### Performing multi-parameter reactions in Magne-Chip.

One syringe (the “substrate syringe”) was filled up through the switching valve (Figure, S-A, S-B, S-F positions) by the adequate substrate from the substrate stocks A-F in accordance to the programmed measurement sequence. Once the substrate syringe (1 mL of volume) was fully loaded the valve switched to S-I position. Substrate, washing buffer or a

mixture of them (mixing ratio is variable from 1:1 to 1:1600) was driven through the chip at a determined flow rate. The internal pressure of the fluid circuitry was continuously monitored through the connector to the other syringe (the “washing buffer syringe”). The chip was kept on a predefined temperature through the measurement.

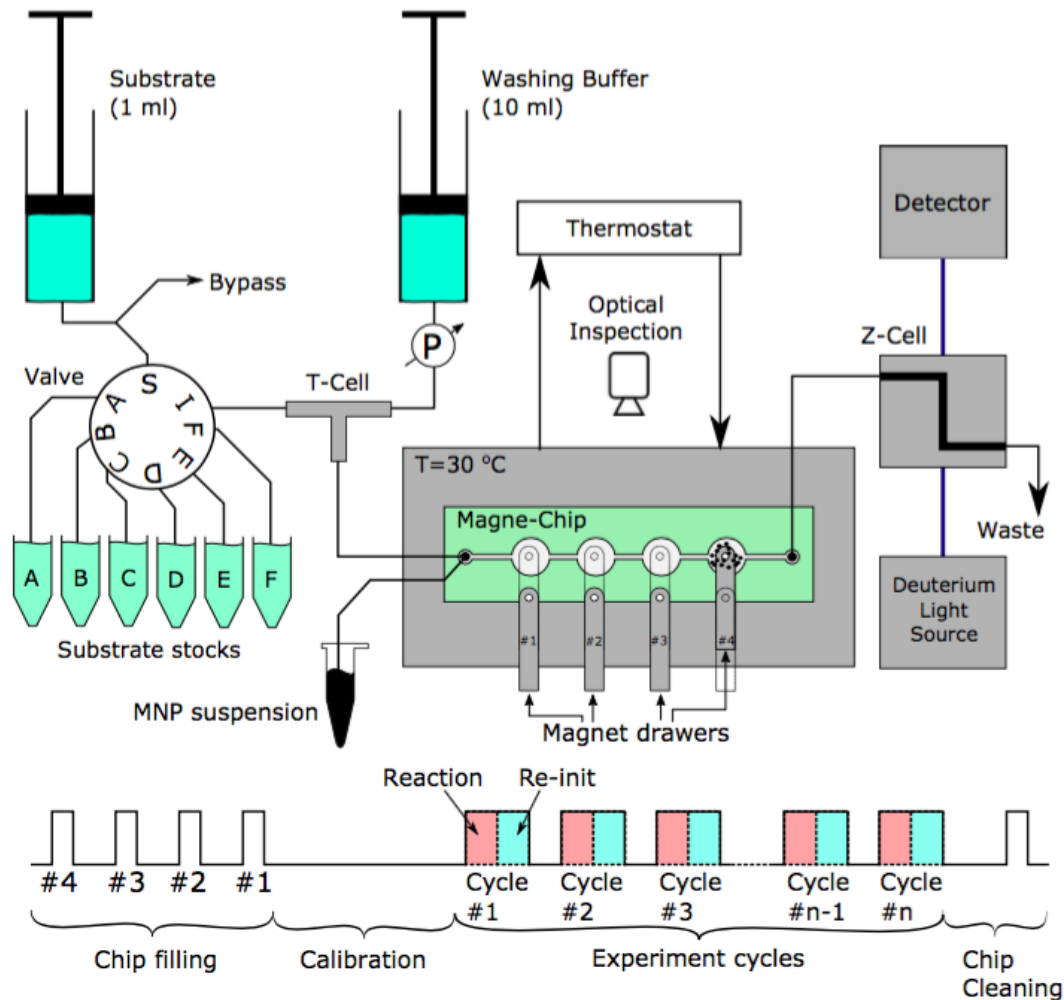


**Figure 1** – Schematic diagram of the fluid control system

### **Experiment cycles**

Each experiment cycle involves a *Reaction step* and a *Re-initialization step* (Figure, Experiment Cycles).

**Reaction step** – (Figure 2,  $t_{end} - t_{start, n+1}$ ) The dosage of the substrate began according to one of the following variants (Table 3, Parameter change). The absorbance value at a previously selected wavelength was continuously monitored. The cycle step ended when the designated step time had been passed or when the reaction had been saturated at least for  $\Delta t_{sat, min} = 10$  min (i.e. absorbance changes fall into the 5% range of the saturation absorbance level) whichever happened earlier.

Variant a) The dosage of the substrate started (1<sup>st</sup> cycle) or continued at unchanged flow rate.

Variant b) The dosage of the substrate started (1<sup>st</sup> cycle) or continued while the flow rate may change cycle by cycle.

Variant c) The dosage of the substrate and the washing buffer ran parallel on a designated ratio resulted in a predefined dilution of the substrate at the chip inlet. The dilution ratio may be different cycle by cycle.

Variant d) The remaining substrate was drained through a bypass valve (Figure). The consequent substrate from the substrate stock (A-F) was loaded into the substrate syringe and the dosage of the substrate began at a predefined flow rate.

**Re-initialization step** – (Figure 2,  $t_{\text{end}} - t_{\text{start},n+1}$ ) The dosage of the substrate stopped while the washing buffer was driven through the system at a designated flow rate. The step ended when the designated step time had been passed or when the absorbance value reached the reference value (i.e. absorbance changes fall into the 5% range of the reference absorbance level) at least for  $\Delta t_{\text{ref},\text{min}} = 10$  min, whichever happened earlier.

The reaction and re-initialization steps constitute one cycle. Cycles are repeated several times (Table 3, No. of cycles) according to the predefined measurement sequence.

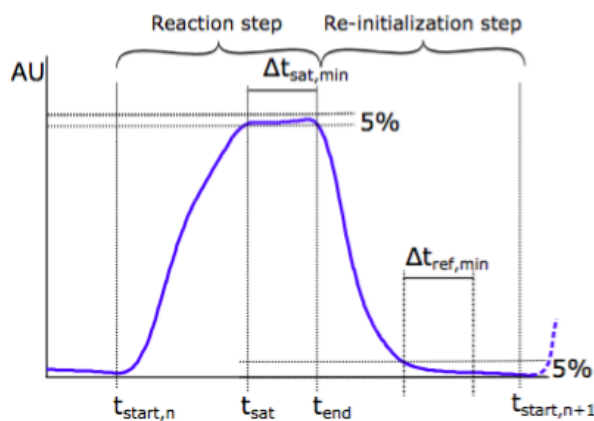


**Figure2** – Typical one cycle absorbance plot over time of multi-parameter measurements in-chip at a given wavelength. Time markers show the integration limits of kinetic calculations. Absorbance markers show the 5% acceptance range of stationary product concentration

## 1.1 Reliability assessment of the measurements

### 1.1.1 General considerations on the measurements in Magne-Chip

As the Magne-Chip system is a quite unexploited tool so far, first the reliability assessment of the measurements was performed. A series of subsequent measurements performed by the system can be considered as reliable if all the following conditions are met:

- the product of the enzyme reaction can be measured selectively in the UV-VIS range;
- product and substrate can be completely removed through the washing steps;
- the enzymatic activity of the MNP biocatalyst remains unchanged during the measurement
- and last but not least, the MNP layer in the magnetic reactors remain unharmed during the measurement cycles.

In order to test the fulfilment of the first group of conditions, a control measurement was done after each experiment i.e. the first step of the sequence was repeated in the last step under the same conditions and the specific activity of the immobilized biocatalyst ( $U_B$ ) at saturation concentrations of L-phenylalanine were compared.

### 1.1.2 Optical inspection of the reaction chambers

During the measurement the chip was optically inspected through a zooming microscope and a monochrome hi-speed smart camera. Before evaluating the measurement sequence, the plan view of the chip was stored as a reference ( $P_{ref}$ ). At the end of the step  $i$  of the measurement sequence the plan view of the chip was sampled again ( $P_{seq,i}$ ) and it was compared to the reference as follows:

$$P_{diff}(j, k) = \begin{cases} P_{ref}(j, k), & P_{ref}(j, k) - P_{seq,i}(j, k) < 0 \\ 0, & P_{ref}(j, k) - P_{seq,i}(j, k) \geq 0 \end{cases}$$

where  $(j, k)$  are the pixel coordinates of the plan view image, therefore the changes in accordance to the reference image are indicated by white pixels. The total sum of white pixels is defined as *cell difference score (SC)* used as a marker for describing the changes of the MNP layer arrangement. Therefore, the changes compared to the image of the first cycle (reference) were indicated by white areas during the consecutive cycles of the measurement.

### 1.1.3 CFD analysis of the reaction cell

The 3D model of a single reaction cell was analyzed. In a certain volume, porous cell zone condition was applied to model the space occupied by the MNPs. Pressure drop was measured in 7 flow rates between  $10 \mu\text{L min}^{-1}$  and  $80 \mu\text{L min}^{-1}$  with and without MNPs in the

chambers, which resulted in  $0.086 \text{ kPa}\mu\text{L}^{-1} \text{ min}^{-1}$  and  $0.059 \text{ kPa}\mu\text{L}^{-1} \text{ min}^{-1}$  flow specific pressure drop, respectively.

Being laminar flow in the channels, the pressure is proportional to the velocity:

$$\text{grad } p = -\mu Dv$$

where  $\mu$  is the dynamic viscosity of the fluid,  $p$  is the measured pressure and  $v$  is the flow velocity at the inlet.  $D$  is the viscous resistance of the porous media (MNP layer). Assuming the parameters of water from the software's material database, it was found that  $D=2.071 \times 10^{10} \text{ m}^{-2}$ .

CFD results are presented in two relevant cases in Figure 3c, d; in the first case the nanoparticle layer fully filled in the chamber, while in the second case the MNP layer is partially destroyed by the unintended passage of an air bubble.

### *Failures of MNP layers detected by visual inspection*

The MNP layer in the magnetic reactors can be damaged due to internal drag forces at higher flow rates and due to air bubble development during the reaction or due to unintended air bubbles from external sources, which may enter the chip during the measurements.

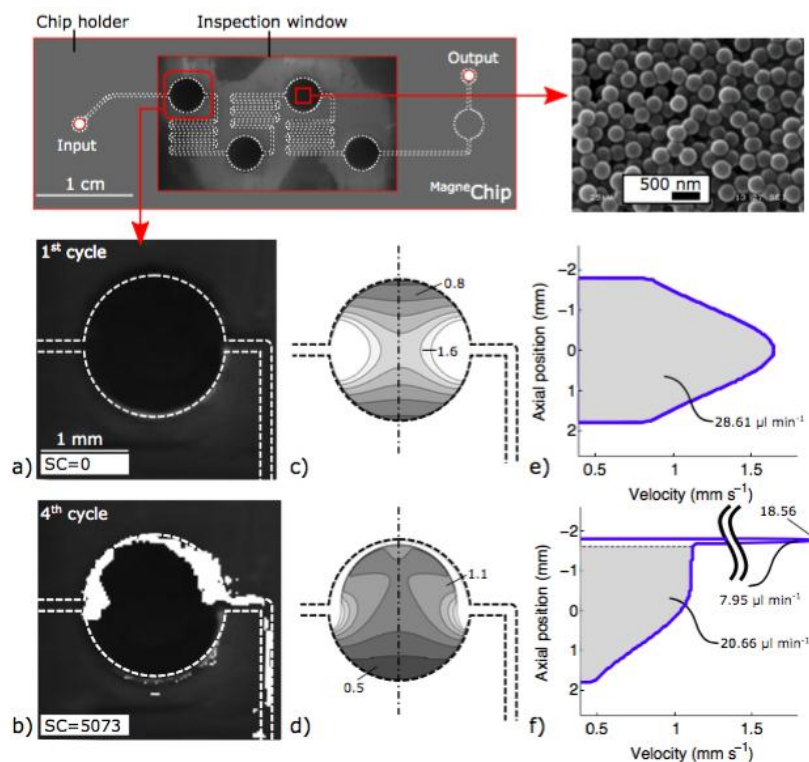


**Figure 3** – Magne-Chip device with four microchambers loaded with MNPs, SEM image of the MNP layer (right). a)-f): The effect of air bubble passage through the reaction cell a) photograph, before passage b) difference image (difference score  $SC=5073$ ), after passage c) calculated flow velocity field before and d) after the passage, e) velocity profile in the middle cross section of the chamber before and f) after the passage

Visual inspection of the chambers provides a continuous measure of significant changes (e.g. bubble passage) of the MNP layer structure. Cell difference score ( $SC$ ) characterizes the actual arrangement of the layer compared to the initial (reference) image. The effect of the air bubble passage can be seen in Figure 3.

In practice,  $SC$  values under 2000 usually reflect negligible changes. However,  $SC > 3000$  may indicate a serious structural change of the MNP layer, for instance the complete breakthrough of a bubble (Figure 3b). Air bubbles usually don't split at the channel entrance, rather pass on one side along the chamber wall. While passing through, the bubble elongates therefore the middle section of the developed tunnel is narrower ( $\sim 300 \mu\text{m}$ ). Numerical simulations revealed (Figure 3c, d, e, f) that the velocity profile became asymmetric due to the bubble passage and the overall mass flow rate through the porous MNP layer significantly decreased ( $28.6 \mu\text{L min}^{-1}$  to  $20.7 \mu\text{L min}^{-1}$ , roughly 72% of its original value) while the remaining fluid passed through the developed tunnel. In the relatively decreased velocity field the substrate concentration may fall below the saturation level. Additionally, the passing bubble may also drift away particles which decreases the sum mass of biocatalysts. Therefore, the biocatalytic activity of the damaged cell decreased and the consequent measurements were no longer reliable.

### ***Assessment of the reliability of the measurements***

Reliability assessment of the measurements was based mostly on the following parameters:

- 1) Cell difference score ( $SC$ ) – Over  $SC > 4000$  (average), the measurement was declined.
- 2) Control measurement – Over 5% of error the measurement was declined.

Table 1 summarizes the assessment evaluation of the measurements.

**Table 1** – Summary of reliability assessment measures.

Experiment	% Error of the control measurement <sup>a</sup> (%)	$SC$ average	$SC$ maximum	Assessment
Multiple fillings, MNP load	3.1	-	-	Accepted
Single parameter cyclic (attempt 1)	1.4	1322	1609	Accepted
Single parameter cyclic (attempt 2)	32.0	4158	5742	Declined
Flow rate optimization	3.2	196	338	Accepted
Substrate screening	1.5	1691	2000	Accepted

<sup>a</sup> Calculation is based on the ratio of the saturation  $U_B$  values of the first and last (control) measurement

## 1.2 Reproducibility of the individual measurements

### 1.2.1 Suspension homogeneity and the effect of filling the chambers with MNP

Biotransformation of L-phenylalanine (**L-1a**) to (*E*)-cinnamic acid (**2a**) by MNP biocatalyst suspension (Scheme 1) was performed in shake vial in three parallel independent cases and resulted in  $U_B = 2.91 \pm 0.08 \mu\text{mol g}^{-1} \text{min}^{-1}$  ensuring that the homogeneity of the MNP suspension was sufficient.

One chamber of the Magne-Chip was filled by applying a magnetic field of a small permanent magnet with the same MNP suspension and the same reaction was performed in flow-through mode and monitored by on-line UV-VIS. The magnet of the chamber was released afterwards and the MNPs were collected in the next chamber. The experiment was repeated three times resulting in  $U_B = 8.01 \pm 0.14 \mu\text{mol g}^{-1} \text{min}^{-1}$ .

The results suggest, neither that the homogeneity of the MNP suspension nor the filling procedure of the chambers had remarkable effect on the reproducibility of the measurements. The significant difference between the  $U_B$  values suggests a more effective reaction in Magne-Chip as compared to the shake vial, though.

Volumetric productivity of the MNP biocatalyst in the chip exceeded the one of the shake vial by more than three orders of magnitude,  $8.82 \text{ g L}^{-1} \text{h}^{-1}$  vs.  $3.13 \text{ mg L}^{-1} \text{h}^{-1}$ , respectively.

### *Re-initialization of the chip and re-use of the MNP biocatalyst in cyclic measurements*

Magne-Chip was filled with MNP biocatalyst and biotransformation of L-phenylalanine **L-1a** to (*E*)-cinnamic acid **2a** was performed in 7 consecutive cycles, while the chip was re-initialized during the steps by washing out the substrate and product completely. The absorbance plot in Figure 4 shows the concentration change of (*E*)-cinnamic acid **2a** at the specific wavelength of 290 nm. It can be clearly seen that the chip was successfully re-initialized in every cycle throughout the experiment and the reaction was repeated seven times, following the same kinetics.

The product quantity was calculated in each cycle. Two independent experiments are shown in Figure 5. In the first attempt (Figure 5, blue bars) the MNP layer remained stable throughout the measurement, resulting in an average product quantity of  $P = 0.12 \pm 1.5\% \mu\text{mol}$ . The moderate mean value of the cell difference score  $SC = 1322$  (1609 max) also reflects negligible changes in the MNP layer. However, the significantly higher mean  $SC = 4158$  (5742 max) in the second attempt (Figure 5, red bars) indicates a damaged MNP layer structure due to an air bubble passage. It is also remarkable that the cyclic product quantity decreased



abruptly as the *SC* value elevated above the critical value. In fact, the air bubble previously stalled (3<sup>rd</sup> cycle) in the reaction cell, finally drifted away leaving a tunnel behind in the 4<sup>th</sup> cycle (Figure 3b).

The above results suggest that provided an undamaged MNP layer an excellent reproducibility can be achieved by the periodical re-initializing of the chip.

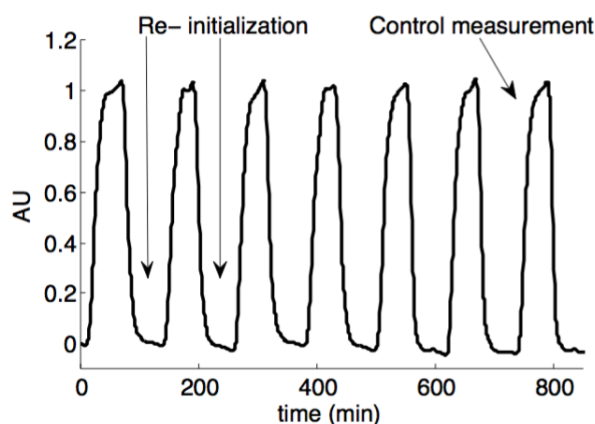


**Figure4**– Time plot of the periodic absorbance change during the cyclic measurement (attempt 1, stable layer). The chip is re-initialized between the reaction steps (reaching zero absorbance) by washing out substrate and product completely. The last measurement acts as a control in each experiment

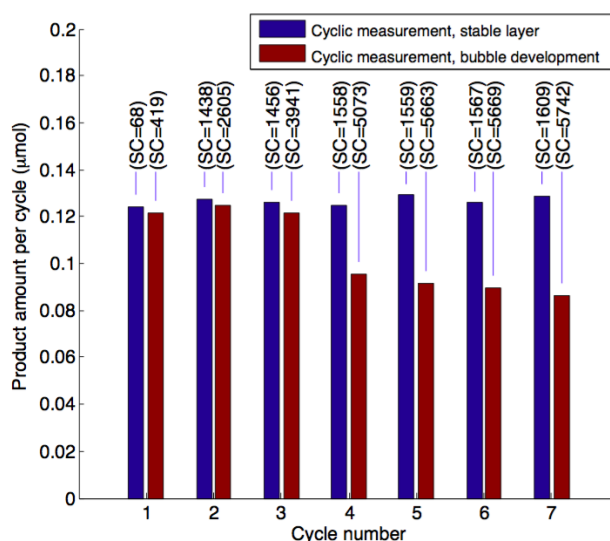


**Figure5**– Product amount *P* per reaction cycle during a cyclic measurement with unmodified parameter settings. Blue bars indicate the attempt with unharmed MNP layer (*SC*<2000) with excellent reproducibility while air bubble passage damaged the layer (*SC*>4000) during the second attempt and demolished the biocatalytic activity (red bars)

### Finding the optimal flow rate for biotransformation with L-1a

Magne-Chip was filled with MNP biocatalyst and biotransformations of L-1a to 2aa were performed in 7 consecutive cycles, while the chip was re-initialized at the end of each cycle and a new substrate flow rate was set. The lowest flow rate was chosen to  $3.6 \mu\text{L min}^{-1}$  and increased in the forthcoming steps up to  $28.6 \mu\text{L min}^{-1}$

(Figure 6). The difference in specific biocatalytic activity ( $U_B$ ) of the reference and control measurements was found to be only 3%, which suggests that the shear forces develop even at the highest chosen flow rate ( $28.6 \mu\text{L min}^{-1}$ ) had not caused irreversible changes on the enzyme activity.

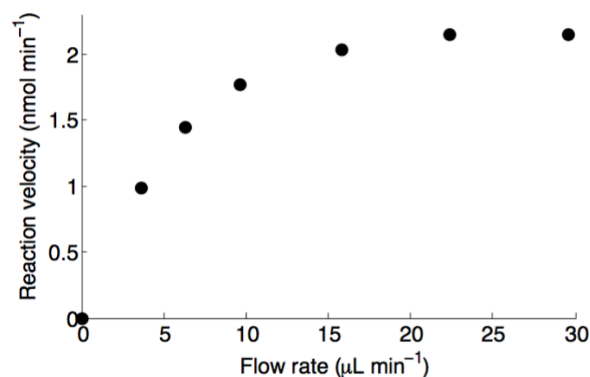


**Figure 6** – Flow rate dependency of the reaction rate in Magne-Chip under the transformation of L-Phe to (*E*)-cinnamic acid by MNP-PAL. Saturation value was achieved at  $25 \mu\text{L min}^{-1}$

The reaction velocity was calculated for each cycles (for details see section 4.2.8 in *Experimental*). By increasing the flow rate, the calculated reaction velocity was increased too, until turned into saturation at about  $25 \mu\text{L min}^{-1}$ .

### Finding the saturation substrate concentration of L-1a

Magne-Chip was filled with MNP biocatalyst and biotransformations of L-1a to 2a at various concentrations of L-1a [S] were performed in 10 consecutive cycles, while the chip was re-initialized at the end of each cycle and a new substrate concentration was set (Figure 7). It was found that the reaction followed the first order kinetics up to [S]=3 mM and saturated roughly at [S]=20 mM.

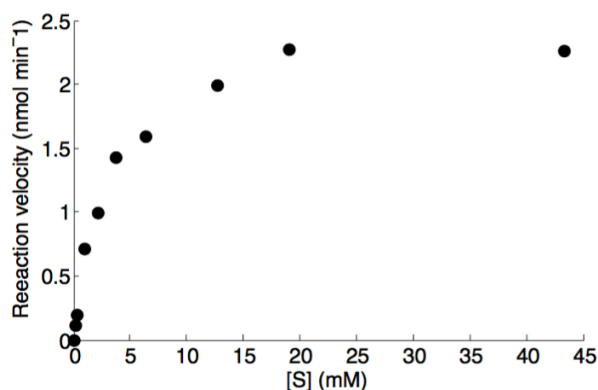


**Figure 7**– Substrate concentration dependency of the reaction velocity in Magne-Chip under the transformation of L-1a to 2a by MNP biocatalyst. Saturation value was achieved at 20 mM

## Substrate screening with MNP biocatalyst in the Magne-Chip system

The screening experiments were performed with the natural substrate (L-**1a**), four different phenylalanine analogues as known substrates of *PcPAL* (*rac*-**1c-f**) and 4-bromophenylalanine (*rac*-**1b**) which has never been tested as substrate for *PcPAL* (Scheme 1). For the substrate screening, the same stock of MNP biocatalyst was as for the previous experiments presented in Sections 2.2–2.4.

First, the extinction coefficients (Table 2) of the corresponding elimination products (**2a-f**, cf. Scheme 1) were determined at selected wavelengths (Figure 8: preferably at wavelengths resulting in high absorbance of the acrylic acid **2** while practically zero of the amino acid **1a-f**) using the flow-cell spectrometer of the Magne-Chip platform. The linear regressions with the measured molar concentration dependence of absorbance values were rather well fitted.

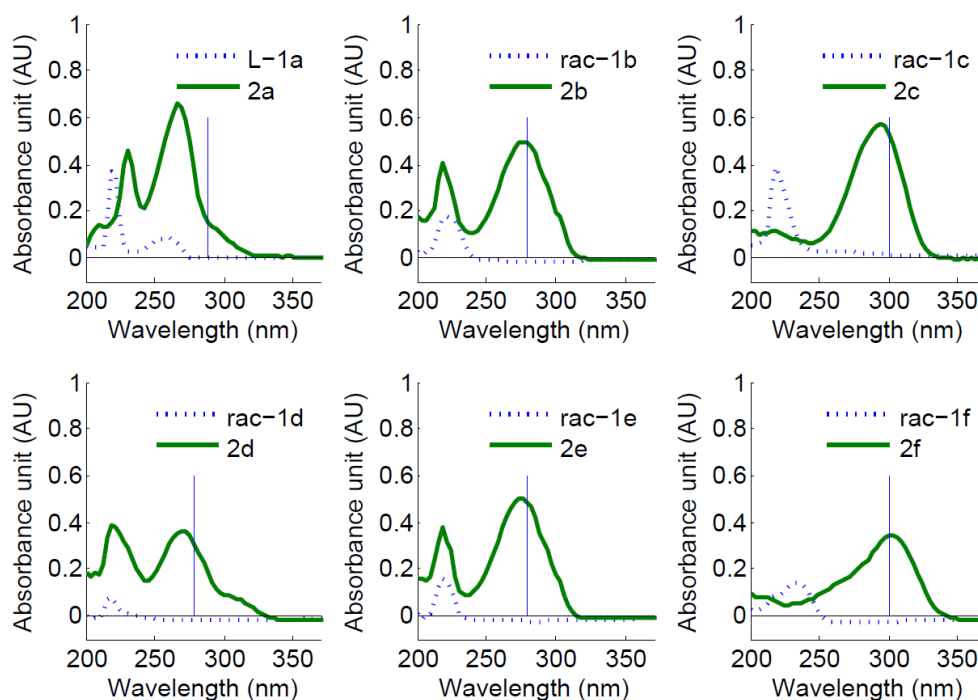


**Figure 8** – Absorbance spectra of L-**1a** and *rac*-**1b-f** (green lines) and the spectra of the corresponding acrylic acids **2a-f** (dotted purple lines). Extinction coefficients were determined at the chosen wavelengths indicated by blue markers

The substrate screening experiments were performed with single chip loading and the different substrate solutions flown through the chip according to a predefined sequence. The intensive washing procedure intended to reach the zero absorbance unit at every relevant wavelengths. In the first cycle the ammonia elimination of *rac*-**1a**, was measured which is the natural substrate of PAL. This case was chosen as reference point of the comparison of the other elimination reaction of PAL substrates. Surprisingly, at high flow rate in the Magne-Chip device, higher biocatalytic activities ( $U_B$ ) were observed for four

of the unnatural substrates (*rac*-**1b,c,e,f**), than for the natural substrate L-phenylalanine L-**1a** (Figure 9).

**Table 2** – Extinction coefficients of the investigated acrylic acids **2a-f**

Acrylic acid	Wavelength (nm)	Extinction coefficient ( $M^{-1}cm^{-1}$ )	Linear regression coefficient
<b>2a</b>	290	8800	0.991
<b>2b</b>	300	10200	0.998
<b>2c</b>	300	7919	0.988
<b>2d</b>	280	14721	0.993
<b>2e</b>	280	9172	0.991
<b>2f</b>	280	15327	0.998

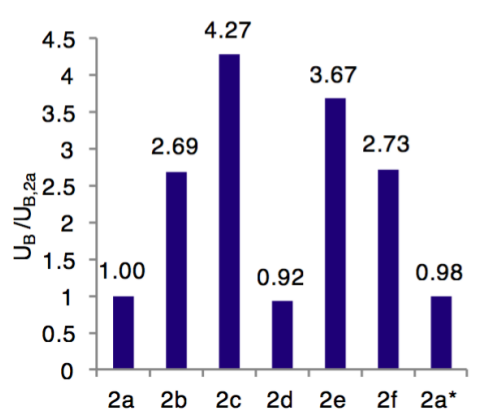


**Figure 9** Comparison of the biocatalytic activity of *PcPAL* enzyme immobilized on MNPs with substrates L-**1a** and *rac*-**1b-f** in Magne-Chip system ([S]= 20 mM, flow rate: 48.6  $\mu L min^{-1}$ ). \* Control measurement

Noteworthy, all the four unnatural substrates showed higher biocatalytic activity ( $U_B$ ) than L-phenylalanine L-**1a** contained slightly more electron-withdrawing aromatic moieties than the phenyl group. This significant deviation from the productivity ranks observed with homogenous *PcPAL* so far<sup>Error! Bookmark not defined.</sup> may be due to the reduced contribution of the reverse reaction (equilibrium effect) to the apparent forward reaction rates in the continuous-flow system at high flow rates.

## Methods

### Immobilization *PcPAL* onto MNPs

Epoxy-MNPs [MagneCat-250GP14 (epoxy-functionalized magnetic nanoparticles with an average diameter of 250 nm): 108 mg] were added to TRIS buffer (3 mL, 0.1 M, pH 8.8) and dispersed by ultrasonication (35 kHz, 20 min). The MNP suspension was added to the *PcPAL* solution (3 mg mL<sup>-1</sup>, in TRIS buffer: 4 mL, 0.1 M, pH 8.8) and the mixture was shaken for 24 h (25 °C, 450 rpm). The PAL-coated MNP particles were fixed at the bottom of the flask with a neodymium magnet and the supernatant was decanted. The MNP preparation was washed – by a re-suspension - magnetic fixing - decantation sequence in each washing

steps – with TRIS buffer ( $3 \times 4$  mL, 0.1 M, pH 8.8) and with ethanol (4 mL). The MNP biocatalyst was dried in vacuum at room temperature for 2 h. After immobilization, negligible protein contents in the supernatants of the washing procedure were determined by the Bradford assay.

### **Microfluidic system with four magnetic microreactor cells (Magne-Chip)**

The reaction with MNP biocatalyst was performed in the magnetic-nanoparticle reactor microchip, consisting of four chambers, 1.1  $\mu$ L of volume each. The chips were made of PDMS (polydimethylsiloxane, Sylgard 184, Daw Corning Ltd, Germany), plasma bonded on a glass substrate. Microchannel dimensions: width 300  $\mu$ m and height 110  $\mu$ m; reaction cell dimensions: volume of 1.1  $\mu$ L, diameter of 3.6 mm, height 110  $\mu$ m<sup>1</sup>.

The chip was fixed in a microfluidic chip holder (Fluidic Connect Pro, MicronitInc, The Netherlands). The microfluidic test bench consisted of two precision syringe pumps, stereo zoom microscope with digital camera, deuterium-halogen light source, spectrometer, Z-flow absorbance cell, circulating thermostat (Julabo Inc. type F-25) and a system controller unit. Gage pressure was measured by MPX4250 (Freescale Semiconductors Ltd., Austin, Texas, US) pressure sensor mounted on the Luer-connector of the syringe (see **Fig. 1**). The system was operated by the  $\mu$ FLU Studio software (developed for the Magne-Chip platform), which controlled the pumps, valves and the thermostat, acquired the data of the chip sensors (e.g. inlet pressure), optically inspected the chip and collected the data of the spectrometer based on the predefined measurement sequence script of the subsequently cases.

### **Filling of the Magne-Chip microreactors with MNPs**

In an Eppendorf-tube a suspension (total volume: 1.5 mL) was prepared from the MNP biocatalyst ( $3.3 \text{ mg mL}^{-1}$ ) and PEG-4000 ( $3.3 \text{ mg mL}^{-1}$ ) in a 5:1 mixture of ultrapure water and 2-propanol. The mixture was sonicated for 15 min in an ultrasonic bath (EMAG EMMI 15HC) kept on 30 °C. Right before the filling up process the suspension was sonicated again for 10 min. During the filling process the chip was kept on 25 °C. To avoid sedimentation gentle shaking (700 rpm) was maintained by an orbital shaker (4.5 mm of orbital diameter) during the chip loading procedure. Neodymium magnets (type N48,  $3 \times 4$  mm) were placed in moveable drawers enabling “on/off” switching of the magnetic field when placed directly below the magnetic cells.

For the optical inspection of the chip the NI-1772 (National Instruments, USA) smart camera was used mounted to a stereo zoom microscope (10 $\times$  magnification).

## Cleaning the chip

Detergent solution (1:99 mixture of EMAG EM-080 and ultrapure water) was used for the cleaning of microchannels. At the end of the reaction, by positioning the moveable drawers to “off” position, the magnetic field is deactivated and TRIS buffer (0.1 M, pH 8.8), solution of detergent, finally ultrapure water were driven through the chip, each for 2 minutes at 300  $\mu\text{L min}^{-1}$  flow rate while the particles were flushed out completely.

## Enzymatic reactions in shake vial

MNP biocatalyst was tested in the ammonia elimination of L-**1a** in shake vials in nine parallel trials. To ensure full homogeneity, MNP biocatalyst (2.0 mg) and PEG 4000 (2.0 mg) were suspended in TRIS buffer (1 mL, 0.1 M, pH 8.8) by sonication for 30 min. In each test reaction 500  $\mu\text{L}$  MNP suspension was added to 500  $\mu\text{L}$  solution of L-**1a** (40 mM in TRIS buffer; 0.1 M, pH 8.8) than the mixtures were shaken in Eppendorf thermoshaker (at 850 rpm, 30 °C) for 20 min. MNPs were collected with magnet, then the product content (**2a**) of the supernatants were determined at  $\lambda = 290 \text{ nm}$  and 30 °C by UV-VIS spectrophotometer (Milton Roy, Genesys 2).

## Enzymatic reactions in Magne-Chip

**Table 3** – Summary of the measurement settings

Experiment	Substrate stocks <sup>1</sup>	Parameter change	Substrate flow rate ( $\mu\text{L min}^{-1}$ )	Washing flow rate ( $\mu\text{L min}^{-1}$ )	No. of cycles <sup>2</sup>	of MNP mass <sup>3</sup> (m g)
Multiple filling of MNP load	<b>A – L-1a</b>	Const. [Var. a)]	48.6 (for 10 min)	440 (for 5 min)	4 (in 1 h)	0.25 (in 1 cell)
Single filling, single parameter	<b>A – L-1a</b>	Const. [Var. a)]	28.6 (for 1 h)	28.6 (for 1 h)	7 (in 14 h)	1 (in 4 cells)
Flow rate optimization	<b>A – L-1a</b>	Flow rate: 3.6-28.6 $\mu\text{L min}^{-1}$ [Varb)]	Varied	28.6 (for 30 min)	7 (in 7 h)	1 (in 4 cells)
Reaction saturation	<b>A – L-1a</b> 3.3 mM <b>B – L-1a</b> 65 mM	[S]: 0.19–43.4mM [Var c)]	28.6 (for 30 min)	28.6 (for 30 min)	10 (in 7 hours)	1 (in 4 cells)
Substrate screening	<b>A – L-1a</b> <b>B – rac-1b</b> <b>C – rac-1c</b> <b>D – rac-1d</b> <b>E – rac-1e</b> <b>F – rac-1f</b>	Substrate [Var d)]	48.6 (for 10 min)	440 (for 10 min)	7 (in 2.3 h)	0.5 (in 2 cells)

<sup>1</sup>When otherwise not stated concentration of substrate was 20 mM. Control measurement in the last cycle was done by the substrate indicated with **bold**.

<sup>2</sup>One cycle constituted Reaction and Re-Initialization steps

<sup>3</sup>Biocatalyst mass was determined as described earlier<sup>1</sup>

Table 3 summarizes the settings of the Magne-Chip platform which were applied during the experiments.

### Calculation of kinetic parameters

Product concentration was calculated by taking the integral of the time dependent absorbance plot at the product specific wavelength:

$$[P](\text{mM}) = \frac{1}{\varepsilon \Delta t} \int_{t_{\text{start}}}^{t_{\text{end}}} A(t) dt$$

where  $\varepsilon$  is the molar extinction coefficient,  $\Delta t$  is the difference of the integration limits.

Product quantity was calculated from the product concentration

$$P(\mu\text{mol}) = [P] \dot{Q} \Delta t$$

where  $\dot{Q}$  is the inlet flow rate.

Biocatalytic activity was calculated by taking the integral of the saturation region of the absorbance plot

$$U_B (\mu\text{mol min}^{-1} \text{g}^{-1}) = \frac{\frac{1}{\varepsilon} \int_{t_{\text{end}}}^{t_{\text{sat}}} A(t) dt \dot{Q}}{m \Delta t}$$

where  $m$  is the total mass of the MNP filling.

Reaction velocity was defined as

$$V(\text{nmol min}^{-1}) = \frac{P}{\Delta t}$$

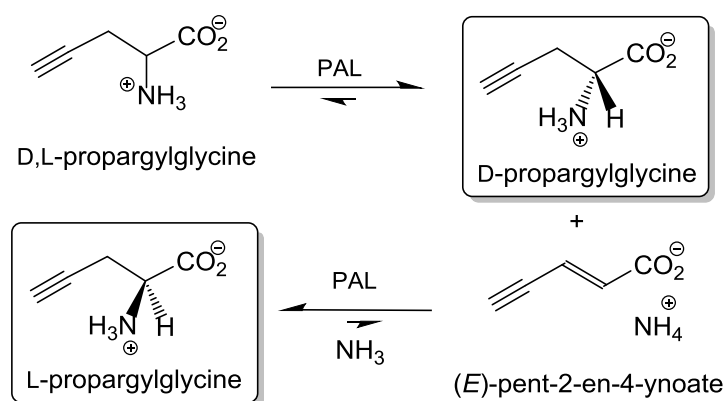
Volumetric productivity was defined as

$$P_V (\text{g L}^{-1} \text{h}^{-1}) = \frac{MP}{V_c \Delta t}$$

where  $M$  is the molar mass,  $V_c$  is the sum volume of the reaction chambers.

### Biocatalytic procedures for the synthesis of non-aromatic alanine derivatives using the Magne-Chip system

Using the previously described system the synthesis of D- and L- propargylglycine was successfully achieved (Scheme 2), obtaining good yield values.



**Scheme 2.** Synthesis of enantiopure D-propargylglycine by PAL-MNPs catalyzed ammonia elimination from D,L-propargylglycine and enantiopure L-propargylglycine by PAL-MNPs catalyzed ammonia addition to (E)-pent-2-ene-4-ynoate.

The construction of the microchip device is depicted in Figure 10.

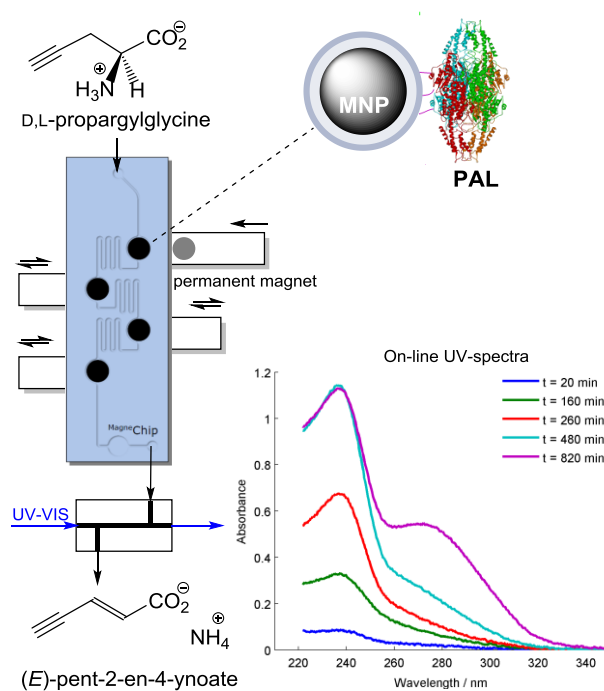


**Figure 10.** The conversion of D,L-propargylglycine in the microfluidic reactor containing the multiple magnetic cells filled with immobilized on magnetic nanoparticles.

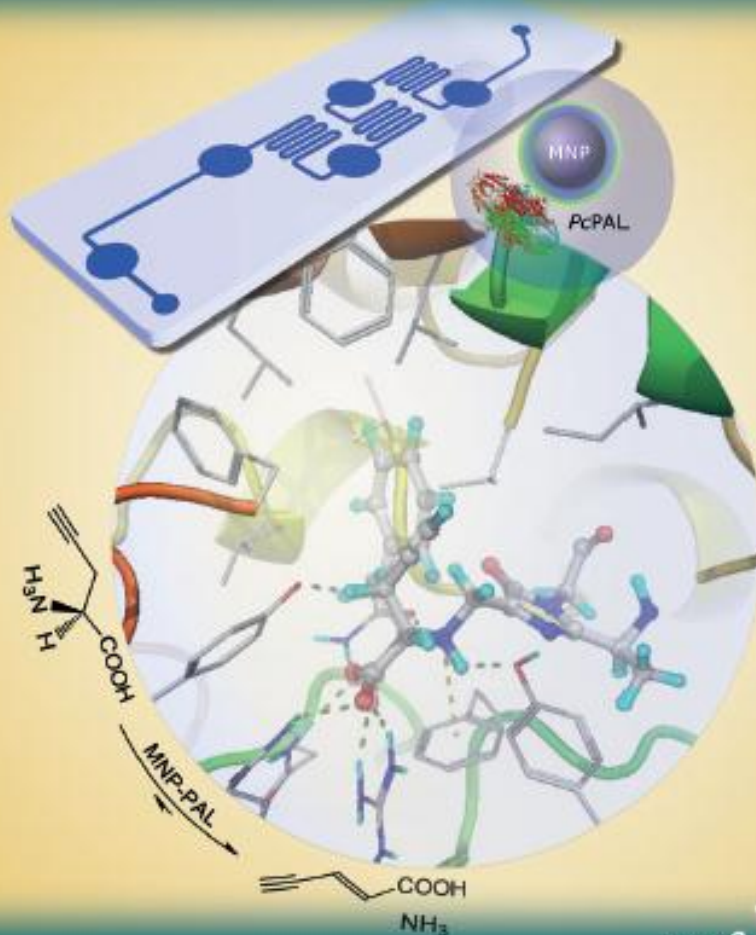
The editorial board of CHEMBIOCHEM journal (where the results were published) has invited the authors of the resulted publication to elaborate the cover page of the corresponding volume (Figure 11).



A EUROPEAN JOURNAL OF CHEMICAL BIOLOGY

# CHEMBIOCHEM

SYNTHETIC BIOLOGY & BIO-NANOTECHNOLOGY



16/2015

Chemistry & Life Sciences

Front Cover:

*C. Paizs, L. Poppe et al.*

Phenylalanine Ammonia-Lyase-Catalyzed Deamination  
of an Acyclic Amino Acid: Enzyme Mechanistic Studies Aided  
by a Novel Microreactor Filled with Magnetic Nanoparticles

WILEY-VCH

[www.chembiochem.org](http://www.chembiochem.org)

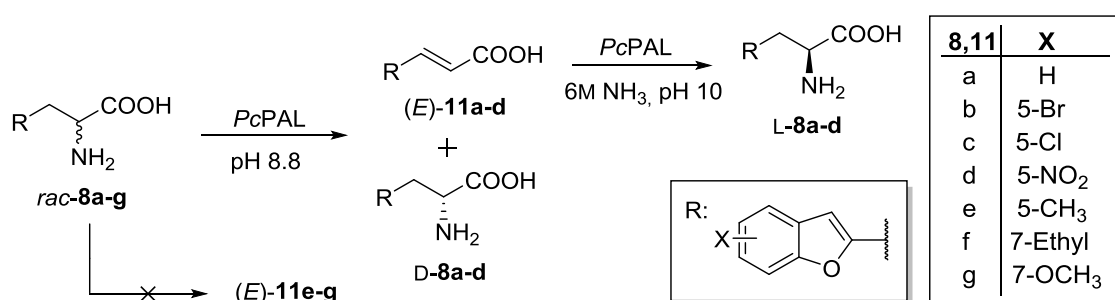
A Journal of



Figure 11. Cover page of Journal CHEMBIOCHEM, volume 16, 2015.

## Biocatalytic synthesis of benzofuranyl derivatives mediated by PAL immobilized on carbon nanotubes

The previously synthesized benzofuranil alanines and their corresponding acrylic derivatives were subjected to the PAL mediated biotransformations using the immobilized form of the enzyme. The result show that the non-substituted benzofuran derivative as well as the ones substituted with electronwithdrawing groups are accepted as substrates by the PAL enzyme, while the derivatives bearing electrondonating groups as substituents are competitive inhibitors for the PAL.



**Table 4** .Enantiomeric excesses and optical rotations of the synthesized L- and D- amino acids

Substrate	Product	ee (%)	$[\alpha]_D^{20}$ (10 mg×mL <sup>-1</sup> ) <sup>a</sup>
<i>rac</i> -8a	D-8a	98	+14,4
<i>rac</i> -8b	D-8b	>99	+31,0
<i>rac</i> -8c	D-8c	>99	+29,3
<i>rac</i> -8d	D-8d	>99	+21,2
( <i>E</i> )-11a	L-8a	>99	-14,5 <sup>8b</sup>
( <i>E</i> )-11b	L-8b	>99	-30,8
( <i>E</i> )-11c	L-8c	>99	-29,1
( <i>E</i> )-11d	L-8d	>99	-21,3

<sup>a</sup>in CH<sub>3</sub>COOH, at 20°C

## Biocatalytic synthesis of alanine derivatives using whole-cell mediated biotransformations

Further we investigated the possibility to perform the biotransformations of the previously described substrates using intact whole-cells of E.coli, expressing PAL enzyme. The batch experiments using the cell suspension proved to have lower efficiency than those employing the native enzyme, probably due to the transfer-transport problems occurring at the cellular membrane. Immobilization of the cells in alginate or silica matrixes were inefficient, due to their structural instabilities at

alkaline pH (the ammonia elimination reaction is performed at pH of 8.8, while the ammonia addition reactions employs the use of 6M, pH 10 ammonia solutions). The use of reticulation reactants produced immobilized whole-cells with 300 fold decreased activity in comparison with the non-immobilized cells.

## Conclusion

A microfluidic device was characterized consisting of several microliter volume reaction chambers filled with magnetic nanoparticles coated with immobilized phenylalanine ammonia-lyase as functional biocatalyst. The chip could be operated cyclically.

It was shown that neither the homogeneity of the MNP suspension nor the filling procedure of the chambers had remarkable effect on the reproducibility. It was also found that the product quantity of cyclically repeated measurements deviate only 1.5% around the mean in a 14 h timeframe.

During cyclic operations, optical inspection of the MNP layer and repeated control measurements offered measures to assess the reliability of the operation. The visible degradation of the layer was described by the arbitrary *SC* value (cell difference score, i.e. by quantification of the missing part of the original MNP layer). The effect of bubble passage was investigated experimentally and by numerical methods as well. It was found that air bubbles had serious effect on reproducibility and also increases the *SC* value. The deviation of the biocatalytic activity of first and the last cycles was also evaluated in each series of experiments (the difference was only in the 1.4–3.6% range in the accepted cases).

Saturation flow rate and substrate concentration of the in-chip transformation with L-phenylalanine **L-1a** to (*E*)-cinnamic acid **2a** were found to be 25  $\mu\text{L min}^{-1}$  and 20 mM, respectively.

The usefulness of the Magne-Chip system for automated activity screening, a cyclic test series was performed. In this study, four known (*rac*-**1c-f**) and a novel (*rac*-**1b**) unnatural substrate of *PcPAL* were tested for in-chip biocatalytic activity with MNP biocatalyst compared to the natural L-phenylalanine **L-1a** substrate of the enzyme. In a cycle of this series, the solution containing a certain substrate candidate flown through the chip and the product concentration was measured in an UV-VIS flow cell. After reaching the stationary state with the actual test substrate, the chip was re-initialized by washing out the reagents, while the MNP loading remained in the reaction chambers. The cycle was repeated afterwards with different substrates. It was found that four of the five unnatural substrates

(*rac*-**1b,c,e,f**) exceeded the biocatalytic activity of the natural substrate (*L*-**1a**). In case of the 2-furanyl analogue (*rac*-**1c**), 4.27 fold activity enhancement compared to *L*-**1a** was achieved.

*As conclusion, it was proved that the Magne-Chip microfluidic device is a reliable, reproducible and efficient tool which was capable of fast, reliable and fully automated screening of PcPAL substrates (and a potential substrate candidate) with minimal solvent (~500 µl) and biocatalyst (~1 mg MNP) usage for a test compound. Compared to shake vial, the volumetric productivity of the MNP biocatalyst in the chip exceeded the one of the shake vial by more than three orders of magnitude.*

*The same device was successfully used for the synthesis of D- and L- propargylglycine. PAL immobilized on carbon nanotubes proved to be an efficient catalyst for the synthesis of D- and L-benzofuranil alanines bearing and electronwithdrawing group on the heterocyclic moiety.*

*Whole-cell mediated biotransformations proved to be unefficient, it is not recommended their use, as suspension or in their immobilized forms in the preparative scale synthesis*

## Selective literature

1. Poppe, L.; Paizs, C.; Kovács, K.; Irimie, F. D.; Vértessy, B. G. *Meth. Mol. Biol.* **2012**, 794, 3–19.
2. Hodgins, D.S. *J. Biol. Chem.* **1971**, 246, 2977–2985.
3. Sarkissian, C. N.; Gámez, A. *Mol. Gen. Metab.* **2005**, 86, 22–26.
4. Hughes, A. *Amino Acids, Peptides and Proteins in Organic Chemistry Volume 1. Weinheim Germany: Wiley VCH.* **2009**, p. 94. ISBN 9783527320967.
5. Sheng, J.; Zhang, L.; Lei, J.; Ju, H. *Anal. Chim. Acta* **2012**, 709, 41–46.
6. Wang, M. S.; Black, J. C.; Knowles, M. K.; Reed, S. M. *Anal. Bioanal. Chem.* **2011**, 401, 1309–1318.
7. Song, Y. S.; Shin, H. Y.; Lee, J. Y.; Park, C.; Kim, S. W. *Food Chem.* **2012**, 133, 611–617.
8. He, P.; Greenway, G.; Haswell, S. J. *Microfluid. Nanofluid.* **2010**, 8, 565–573.
9. Gijss, M. A. M.; Lacharme, F.; Lehmann, U. *Chem. Rev.* **2010**, 110, 1518–1563.
10. Weiser, D.; Bencze, L. C.; Bánóczy, G.; Ender, F.; Kókai, E.; Szilágyi, A.; Vértessy, B. G.; Farkas, Ö.; Paizs, C.; Poppe, L. *ChemBioChem* **2015**, doi:10.1002/cbic.201500444
11. Paizs, C.; Katona, A.; Rétey, J. *Chem. Eur. J.* **2006**, 12, 2739–2744.
12. Paizs, C.; Katona, A.; Rétey, J. *Eur. J. Org. Chem.* **2006**, 1113–1116.
13. Gloge, A.; Zoň J.; Kővári, Á.; Poppe, L.; Rétey, J. *Chem. Eur. J.* **2000**, 6, 3386–3390.
14. Bradford, M. M. *Anal. Biochem.* **1976**, 72, 248–254.
15. Bartha-Vati, J. H.; Tosa, M.I.; Irimie, F.D.; Weiser, D.; Boros, Z.; Vértessy, B.; Poppe, L.; Paizs, C. *ChemCatChem* **2015**, 7, 1122–1128.
16. Ender, F.; Weiser, D.; Nagy, B.; Bencze, L.C.; Banoczy, G.; Ender, F.; Kiss, R.; Kokai, E.; Szilágyi, A.; Vértessy, B.; Farkas, O.; Paizs, C.; Poppe, L. *ChemBioChem* **2015**, 16, 22983–2288